32nd Annual International Conference of the IEEE EMBS
Buenos Aires, Argentina, August 31 - September 4, 2010

SAR Evaluations of Mobile Phone Close to a Pacemaker Implanted in Human Body

Ryohei WATANABE[1], Kazuyuki SAITO[2, 1], *Member*, *IEEE*, Soichi WATANABE[2], *Member*, *IEEE*,
Masaharu TAKAHASHI[1], *Senior Member*, *IEEE*, Koichi ITO[1], *Fellow, IEEE*

***Abstract*—Recently, electromagnetic interference (EMI) of an implanted pacemaker with a mobile phone was largely investigated. As for the pacemaker, the Japan National Authorities have recommended to keep the mobile phone in safe distance from the cardiac pacemaker. Meanwhile, evaluation of the interaction between the electromagnetic (EM) wave and human body was in progress. Therefore, the absorption of EM energy to the human body especially around the pacemaker, where the mobile phone was in a chest pocket of the pacemaker holder, was thoroughly evaluated. We provided the calculation of specific absorption rate (SAR) distributions around the pacemaker model that implanted into a rectangular parallelepiped torso model, when a mobile phone model is placed in the vicinity. In addition, the SAR was also experimentally performed to validate the such numerical calculations. We confirmed that SAR distributions could be estimated from the presence or absence of pacemaker model. Moreover, the measurement results of the SAR distribution suited to the calculation, thus its validation was achieved.**

I. Introduction

Implanted cardiac pacemaker is one of the most significant devices used for treatment of cardiac arrhythmia. The pacemaker system monitors the pulses of the heartbeat through an implanted electrodes and stimulates the heart by voltage pulses if a slow arrhythmia is detected.

Recently, the electromagnetic interference (EMI) of the pacemaker from mobile phone has widely been investigated [1]-[3]. These investigations shown that the electromagnetic waves caused interference to internal electronic circuits through the connector between the pacemaker housing and the lead wire of the electrode. Therefore, the connector played a major role for the EMI due to the mobile phones. In this case, a pacemaker acted as a receiving antenna with respect to the EM waves from the mobile phone. In order to avoid the EMI, national authorities have recommended to keep the mobile phone in safe distance from the cardiac pacemaker [4].

Incidentally, mobile phone may be close to an implanted pacemaker when the patient gets on a crowded train, or accidentally puts a mobile phone in own chest pocket. In this case, besides the EMI of the pacemaker, the absorption of electromagnetic (EM) energy in the human body especially around the pacemaker must be considered, owing to the contribution of EM waves to the heat effect.

The specific absorption rate (SAR) is usually used for the primary dosimetric parameter of the EM wave exposure for standardization [5], expressed as:

$$\mathrm{SAR} = \frac{\sigma E^2}{\rho} \quad [\mathrm{W/kg}] \tag{1}$$

where, σ [S/m] is conductivity of tissue, r [kg/m^3] is density of tissue, and E [V/m] is electric field strength within tissue.

In this paper, SAR due to a PIFA (planar inverted F antenna) mounted on a metallic case for third generation mobile phone around a pacemaker implanted in a rectangular torso model is simulated by the FDTD (finite difference time domain) method. Then, the validity of the calculated results is experimentally confirmed by the thermographic method.

II. Numerical Analysis

Figures 1 (a) and (b) show the PIFA mounted on the metallic case and S_{11} characteristics of the antenna in free-space, respectively. Fig. 1 (b) indicates that the PIFA satisfactorily resonates at 2 GHz. The solid line is the calculated result and the dash line is the measured result. Good agreement between measurement and calculation is achieved. Figure 2 shows a pacemaker model. The model referenced to [6]. The pacemaker housing has a dimension of $40 \times 30 \times 6$ mm^3 with a lead wire has a diameter of 2 mm and its length of 240 mm. The electrode is inserted into the heart to detect a myocardial potential. Its dimension is $6 \times 6 \times 6$ mm^3.

Figure 3 shows our model for numerical calculation. The pacemaker model is implanted in a rectangular torso phantom and a PIFA mounted on a metallic case in the vicinity of the torso. The PIFA is operated at 2 GHz and the output power is set by 0.25 W. Here, the torso is simplified as a rectangular parallelepiped, whose electrical properties are the same as the human muscle [7]. The properties are as follows - relative permittivity ε_r = 54.2, conductivity σ = 1.5 S/m at 2 GHz, and density ρ = 1,040 kg/m^3. The PIFA is kept at a distance of 15 mm from the surface of the torso model. The distance is decided by referring to [8]. Moreover, the PIFA is located in z (Fig.4(a)) and x directions (Fig.4(b)) to investigate the dependence of the metallic case direction. Table. I lists the parameters for the FDTD calculations.

[1] The author is with Chiba University, Inage-ku, Chiba, Japan
[2] The author is with National Institute of Information and Communications Technology, Koganei, Tokyo, Japan.

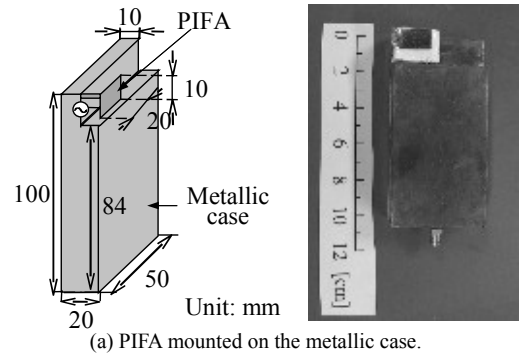

(a) PIFA mounted on the metallic case.

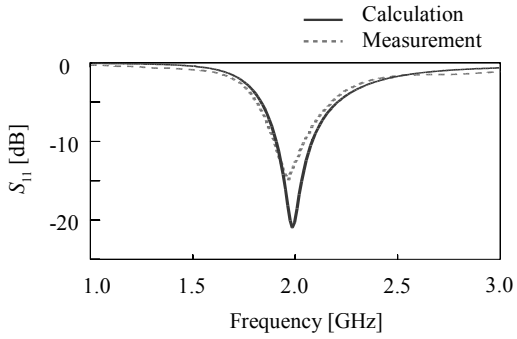

(b) S_{11} characteristics of the PIFA in free-space.

Fig. 1. Mobile phone model.

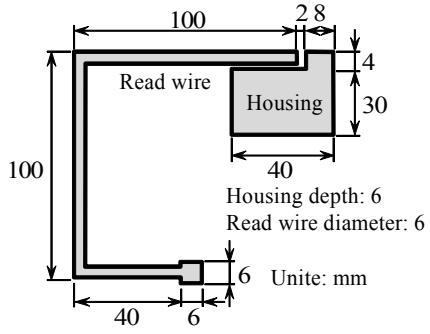

Fig. 2. Pacemaker model.

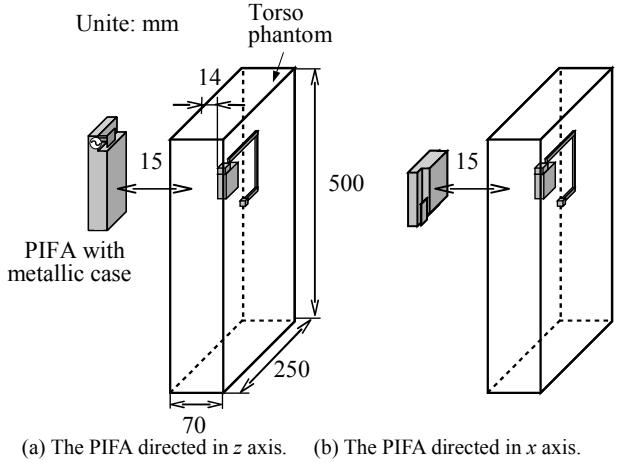

(a) The PIFA directed in z axis. (b) The PIFA directed in x axis.

Fig. 3. Numerical calculation models.

TABLE I

PARAMETERS FOR FDTD CALCULATIONS.

Analytical space $x \times y \times z$ [cell]	400 × 400 × 400	
Cell size [mm]	Δx, Δz	2.0
	Δy	1.0
Time step [ps]	2.7	
Absorbing boundary condition	PML (8 layers)	

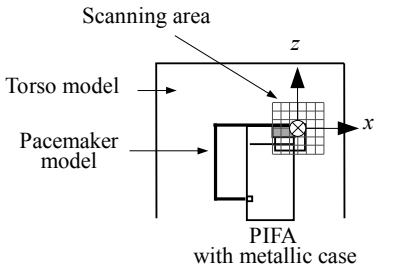

(a) PIFA direction: z axis.

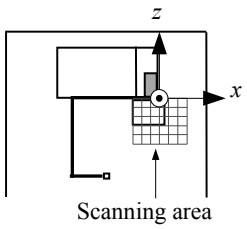

(b) PIFA direction: x axis.

Fig. 4. Scanning area of feeding point.

III. NUMERICAL RESULTS

Upon calculating SAR around the pacemaker model, the PIFA is scanned in x-z plane. Figure 4 shows the scanning area of feeding point of the PIFA mounted on the metallic case. The SAR is calculated when a feeding point of the PIFA is faced with each grid point in Fig. 4. In addition, the SAR on each position converted into 10-g averaged SAR (ref. [9]). Here, 10-g averaged SAR is defined in the value in which local SAR is averaged by 10 g tissue.

Figure 5 depicts maximum values of 10-g averaged SAR on each position in the scanning area. These maximum values of 10-g averaged SAR are observed at the torso surface on each position. Fig. 5 (a) shows maximum value at x= z= 0 mm. It is that the feeding point of the PIFA faced with the gap of pacemaker model. According to Fig. 5 (b), the maximum value is observed at x= 10, z= -30 mm. It is that the lead wire directed toward x axis faced with the center of the metallic case of the PIFA. Comparing Figs. 5 (a) with (b), both of maximum value is 1.36 W/kg. Hence, there is not dependence of the PIFA directions. Fig. 6 shows SAR distribution in y-z plane (x=0). According to Fig. 6 (a), a standing wave is observed between the torso surface and the pacemaker model. It is because the SAR around implanted pacemaker is higher compared with the model without pacemaker.

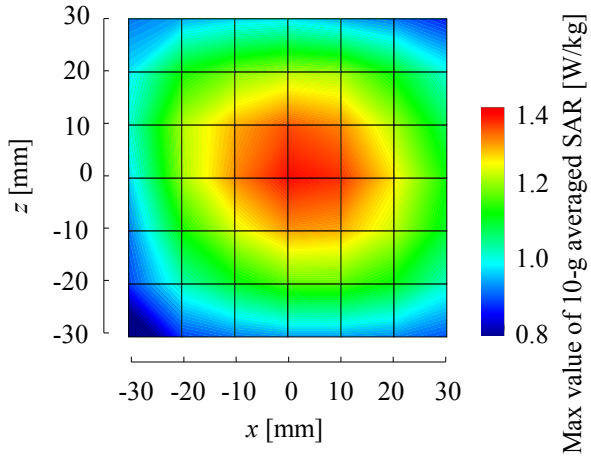

(a) PIFA direction: z axis.

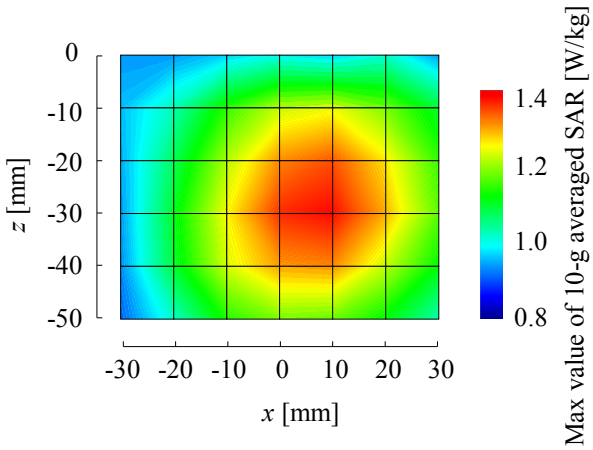

(b) PIFA direction: x axis.

Fig. 5. 10-g averaged SAR in each position.

As earlier mentioned, when a conductor was implanted in the human body, SAR around the conductor increased. It was confirmed in [10] as well as our results. In fact, 10-g averaged SAR have been limited in less than 2 W/kg by the guideline on human exposure to EM fields in Japan. In addition, when the conductors were implanted into the human body, the guideline indicated that the possibility of the exposure below the guideline value might cause a local heating. Thus, the guideline value (i. e. 2 W/kg) was not applied in this case. However, as increasing number of pacemaker user, such a case must be applied to the guideline[11]. Therefore, the influence on SAR by the implanted conductors have to be investigated in detail [12].

IV. Experimental Validations

The SAR is also experimentally evaluated to validate the numerical calculations. Fig. 7 shows experimental set up for thermographic method [13]. In the SAR measurement, sinusoidal wave of approximately 100 W is fed to the PIFA mounted on the metallic case. Following the short time exposure, the temperature rise is taken by thermographic camera. The SAR at observation plane is defined by the following equation:

$$\mathrm{SAR} = C\frac{\Delta t}{\Delta T} \quad [\mathrm{W/kg}] \tag{2}$$

where C [J/kgK] is specific heat of the phantom, ΔT [K] is temperature rise, and Δt [s] is exposure time.

The observation plane is sagittal plane between the torso surface and the pacemaker model. Fig. 8 shows measured and calculated SAR distribution on the observation plane. Both results are normalized by the maximum value of each SAR. Figs. 8 (a) and (b) describe two local maximum values in front of pacemaker model for both measured and calculated results, respectively. The maximum value is observed at the torso surface whereas the local maximum value is noticed in front of the pacemaker model.

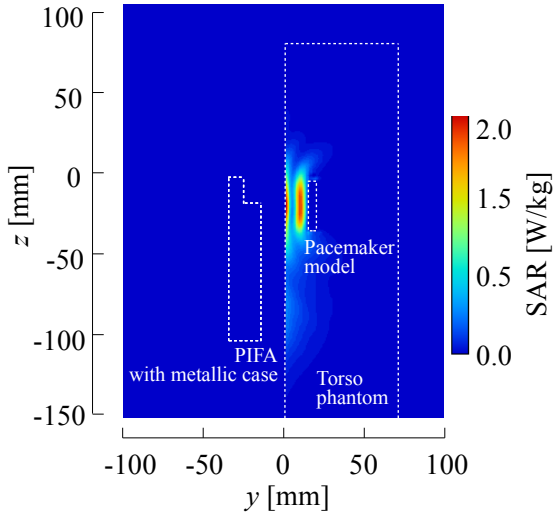

(a) SAR distribution with pacemaker model.

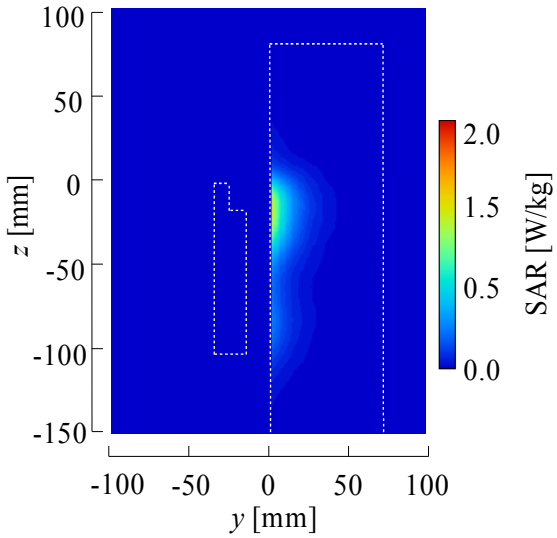

(b) SAR distribution without pacemaker model.

Fig. 6. Dependency of SAR distributions on presence or absence of the pacemaker model.

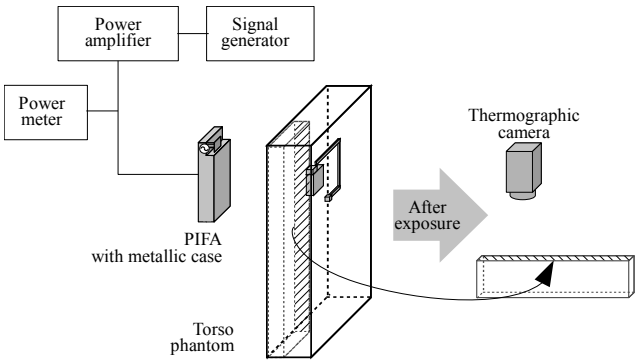

Fig. 7. Experimental set up.

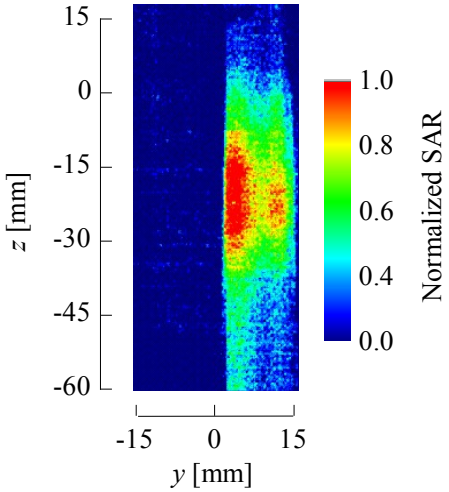

(a) Measured result.

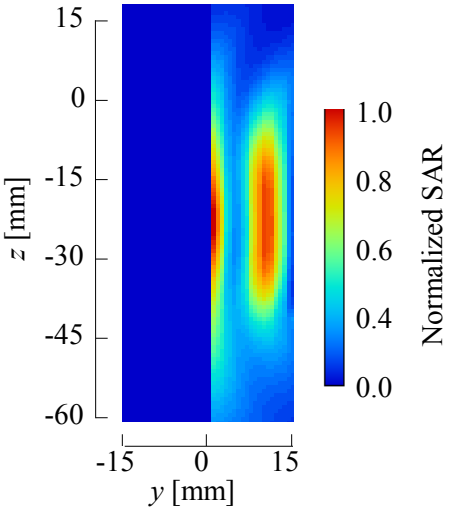

(b) Calculated result.

Fig. 8. SAR distributions in front of pacemaker model.

V. Conclusions

10-g averaged SAR around the pacemaker model implanted into a torso phantom was calculated when the PIFA mounted on the metallic case was placed in vicinity of the torso. The difference of the SAR distribution was confirmed upon the presence of the pacemaker model. This tendency has also been validated by the measurement. As for further investigations, the torso phantom will be replaced with a realistic human model for calculations of the SAR.

References

[1] Irnich W. "Interference in Pacemaker," *PACE*, vol. 7, pp. 1021-1048, 1984.

[2] S. Stefan, LO. Fichte, and S. Dickmann, "EMC Modelling of Cardiac Pacemakers," in *proc. 18th Int. Zurich Symposium on EMC*, pp. 33-36, Sep. 2007.

[3] AK. Lee, and JK. Pack, "Study of the Tissue Volume for Spatial-Averaged SAR Evaluation," *IEEE Tras. Electromagnetic Compatibility*, Vol. 44, No. 2, pp. 404-408, May 2002.

[4] "Guidelines on the Use of Radio communication Equipment such as Cellular Telephones -Safeguards for Electronic Medical Equipment- ," *EMC Conference Japan*, Electromagnetic Medical Equipment Study Group, 1997.

[5] *IEEE Standard for Safety Levels with Respect to Human Exposure to Radio Frequency Electromagnetic Fields*, 3 kHz to 30 GHz, 1999.

[6] J. Wang, O. Fujiwara, and T. Nojima, "A Model for Predicting Electromagnetic Interference of Implanted Cardiac Pacemakers by Mobile Telephones," *IEEE Trans. Microw. Theory Tech.*, Vol. 48, No. 11, pp. 2121-2125, Nov. 2000.

[7] C. Gabriel, "Compilation of the dielectric properties of body tissues at RF microwave frequencies," *Brooks Air Force Technical Report* AL/OE-TR-1996-0037, 1996.

[8] Federal Communications Commission. Evaluate Compliance with FCC Guidelines for Human Exposure to Radiofrequency Electromagnetic Fields Office of Engineering & Technology. OET Bullentin 65, Eddition 97-01, June 2001.

[9] IEEE Recommended practice for measurements and computations of radio frequency electromagnetic fields with respect to human exposure to such fields, 100 kHz-300 GHz; IEEE Standard C95.3-2002, 2003.

[10] H. Virtanen, J. Huttunen, A. Toropainen, and R Lappalaiainen, "Interaction of mobile phones with superficial passive metallic implants," *Physics in Medicine and Biology*, vol. 50, pp. 2689-2700, 2005.

[11]C. R. Roy, "Rapporteur report: ICNIRP international workshop on EMF dosimetry and biophysical aspects relevant to setting exposure guidelines," *Health Phys.*, vol. 92, no. 6, pp. 658-667, 2007.

[12]International Commission on Non-Ionizing Radiation Protection, "Exposure to high frequency electromagnetic fields, biological effects and health consequences (100 kHz-300 GHz) - review of the scientific evidence and health consequences," 2009.

[13]Y. Okano, K. Ito, I. Ida, and M. Takahashi, "The SAR evaluation method by a combination of thermograohic experiments and biological tissue-equivalent phantoms," *IEEE Trans. Microw. Theory Tech.,* vol. 48, no. 11, pp. 2094-2103, Nov. 2000.